## PAPER

# Comparative analysis of chitin isolation techniques from mushrooms: toward sustainable production of high-purity biopolymer†

Akhiri Zannat,[a] Isaac Eason,[b] Benjamin Wylie,[b] Robin D. Rogers, [ID][c] Paula Berton [ID] *[d] and Julia L. Shamshina [ID] *[a,b]

Chitin, an abundant and versatile biopolymer, is widely used across industries such as biomedicine, agriculture, and materials science. Traditionally sourced from crustacean waste, its extraction poses environmental and allergenic challenges, driving the exploration of alternative sources. Fungal biomass, particularly from white mushrooms (*Agaricus* bisporus), offers a renewable, hypoallergenic, and non-animal alternative, but its complex cell wall structure demands innovative extraction techniques. This study compares traditional alkaline pulping with environmentally-conscious methods, including ionic liquids 1-ethyl-3-methylimidazolium acetate ([C$_2$mim][OAc]) and 1-butyl-3-methylimidazolium hydrogen sulfate ([C$_4$mim][HSO$_4$]), and a deep eutectic solvent made of lactic acid and choline chloride (LA : [Cho]Cl), for chitin isolation from mushroom biomass. Results indicate that thermal [C$_2$mim][OAc] and extended NaOH pulping produced isolates with superior purity (77%), retaining the structural integrity of α-chitin. The produced fibers demonstrated mechanical properties of fungal chitin comparable to crustacean-extracted chitin, highlighting the viability of fungal sources for high-value applications. By addressing critical challenges in fungal chitin extraction, this work advances the understanding of eco-friendly methods and their potential for scalability. The ability to source chitin from mushrooms rather than from traditional animal-based sources like crustaceans is a game-changer for ethical and sustainable biomass to C-based products industries. In addition, the findings underscore fungal biomass as a valuable yet underutilized resource in the context of carbon-efficient biomass utilization. Mushrooms grow on various agricultural and industrial wastes, have minimal environmental impact, and their cultivation emits significantly fewer greenhouse gases compared to other agri- and aquacultural processes. In addition, the presented extraction method using [C$_2$mim][OAc] reduces chemical waste compared to traditional alkali-based methods for obtaining fungal chitin. Integrating this type of chitin into numerous applications reduces reliance on traditional supply chains and reinforces a circular economy approach.

### Green foundation
1. This work advances green chemistry by developing eco-friendly extraction methods for chitin from renewable fungal biomass, offering a sustainable alternative to crustacean-derived chitin. It reduces reliance on animal-based sources and minimizes environmental harm, aligning with principles of waste valorization and circular economy.
2. The use of [C$_2$mim][OAc] as a solvent reduces chemical waste compared to traditional alkali-based methods. It achieves high chitin purity (77%) with retained α-chitin structural integrity, comparable to crustacean-sourced chitin. Mushrooms, grown on agricultural waste, further enhance sustainability by minimizing environmental impacts and greenhouse gas emissions.
3. Further research on optimizing energy use during extraction and exploring scalability would elevate the approach for broader industrial adoption.

[a]*Fiber and Biopolymer Research Institute, Department of Plant and Soil Science, Texas Tech University, Lubbock, TX, USA. E-mail: jshamshi@ttu.edu*
[b]*Department of Chemistry and Biochemistry, Texas Tech University, Lubbock, TX, USA*
[c]*525 Solutions, Inc., PO Box 2206, Tuscaloosa, AL 35403, USA*
[d]*Chemical and Petroleum Engineering Department, University of Calgary, Calgary, AB, Canada. E-mail: paula.berton@ucalgary.ca*
†Electronic supplementary information (ESI) available. See DOI: https://doi.org/10.1039/d4gc06388k

# Introduction

Chitin, the second most abundant natural biopolymer, consists of *N*-acetyl-D-glucosamine units linked by β-(1,4) glycosidic bonds. Its unique properties make it widely utilized across various industries.[1] In the pharmaceutical sector, chitin is valued for its biocompatibility and biodegradability, serving as a scaffold material and as an encapsulating vehicle for drug delivery systems.[2,3] In agriculture, it serves as a natural pesticide and fertilizer,[4] while in the food industry, its properties make it an excellent choice for packaging materials.[5,6] These diverse applications position chitin as a promising polymer for further research and development, particularly in sectors aiming for sustainable and eco-friendly alternatives.[7–9]

Crustacean waste, particularly from crabs, shrimp, and lobsters, has traditionally been the primary industrial source of chitin due to its easy availability and high chitin content, which ranges from 8 to 40%. Seafood processing yields significant quantities of this biopolymer, with the global production of crustaceans totaling 15.5 million metric tons (MMT), with shrimp and prawns accounting for 9.7 MMT (62.4%), freshwater crustaceans 3.8 MMT (24.8%), and crabs 2.0 MMT (12.8%).[8,10] Approximately 45–60% of this amount becomes waste after processing.[11] However, the seasonal availability of crustaceans, the presence of allergenic proteins such as tropomyosin, arginine kinase, and others,[12–16] and environmental impacts from processing have prompted the search for alternative sources.

Fungal sources of chitin, particularly mushrooms, are increasingly recognized as promising alternatives due to their non-animal origins and hypoallergenic nature.[17] Mushrooms, which can be cultivated year-round, offer consistent production unaffected by seasonal variations.[18] Moreover, the controlled growth conditions required for fungal cultivation make them a sustainable source of chitin. Mushrooms can be specifically cultivated for chitin production, using biowaste as a cost-effective substrate for growth.[19] Fungal cultivation requires minimal land area, utilizing vertical stacking for growth, and mushrooms typically mature within 2 to 3 weeks. In contrast, crustaceans, such as *Litopenaeus vannamei*, require approximately 12 months to grow.[20] This rapid growth can offset the lower chitin yield per wet weight of the fruiting body compared to crustaceans.

In the context of chitin extraction, it is crucial to understand the structural differences and associated challenges between fungal-derived and crustacean-derived chitin. Crustacean biomass, particularly from shrimp and crab, contains varying levels of chitin, proteins, and minerals, with the remaining mass consisting of astaxanthin and lipids. Shrimp biomass has a chitin content ranging from 15% to 40%, protein levels between 20% and 40%, and a high mineral content of 30% to 60%.[21,22] Similarly, crab biomass contains 25% to 30% chitin, with a slightly lower protein composition of 15% to 20%, while its mineral content ranges from 30% to 50%.[23]

In comparison to crustacean biomass, mushrooms exhibit a broader chitin range depending on the species, from 1.9% (*Lentinellus eoehleatus*)[24] to 44% (*Ganoderma lucidum*)[25] of dry weight. Unlike crustacean chitin, fungal chitin and α-1,3-glucans form a stiff hydrophobic scaffold, embedded within a dense polysaccharide network of β-1,3-, β-1,4-, and β-1,6-glucans,[26] as revealed by solid-state magic angle spinning dynamic nuclear polarization (SS MAS-DNP) nuclear magnetic resonance (NMR) spectroscopy. This structure is further covered by an outer shell containing glycoproteins, linked to structural proteins complicating chitin isolation.[27]

Mushrooms contain 64.8% to 80.0% carbohydrates (including chitin and glucans), 10.5% to 23.3% proteins, 0.6% to 4.4% fatty acids, and 2.8% to 11.0% ash.[28] Unlike crustaceans, which have a high mineral content, mushrooms generally contain lower mineral levels (2.5 to 7.0%).[28,29] However, they are richer in essential micronutrients, particularly potassium, phosphorus, calcium, and magnesium.[28,29] While fungal chitin has a lower mineral content compared to its crustacean counterpart—potentially simplifying some aspects of extraction—the complex cellular structure and the presence of diverse polysaccharides require specialized methods to efficiently separate the chitin.

Chitin isolation from crustacean biomass has traditionally relied on pulping methods using hydrochloric acid (HCl) and sodium hydroxide (NaOH) to remove minerals and proteins.[30–33] However, these processes often involve high temperatures (80–90 °C) and strong alkaline conditions, which can degrade the chitin structure and impact its quality. To mitigate this, researchers have explored milder extraction conditions by reducing temperature and chemical concentrations or replacing mineral acids with weaker organic acids such as acetic and propionic acid.[34–36] While these modifications improve sustainability, they still require significant chemical input and generate waste streams.

To address these limitations, alternative green extraction methods have been developed, including Ionic Liquids (ILs)[37] and Deep Eutectic Solvents (DESs).[38] ILs offer both extraction and pulping approaches. Extraction refers to selective dissolution of chitin leaving behind proteins and minerals. "Pulping" ILs function as dual-action demineralization and deproteinization agents, reactively removing crustacean protein-mineral matrix while preserving the integrity of chitin. DESs, formed from hydrogen bond acceptors (*e.g.*, choline chloride) and hydrogen bond donors (*e.g.*, organic acids, urea), act similarly to "pulping" ILs, facilitating chitin isolation without its dissolution while operating under milder conditions. Both IL- and DES-methods have been extensively reviewed.[37,38] The best "extracting" IL is 1-ethyl-3-methylimidazolium acetate ([C$_2$mim][OAc]) although numerous ILs are known,[37] whereas "pulping ILs" include 2-hydroxyethyl-ammonium acetate [NH$_3$(CH$_2$)$_2$OH][OAc], hydroxylammonium acetate [NH$_3$OH][OAc], *etc.*

As research advances, a few other methods have become available for chitin extraction. One such approach is atmospheric-pressure dielectric barrier discharge (DBD) plasma treatment, which was utilized as an efficient and rapid method for protein removal from crustacean shell waste.[39] While the

method is still in its early stages, its environmental benefits and potential cost savings make it an attractive alternative to conventional chemical-based methods. The electricity-driven separation process appears to be scalable (with further development, particularly in continuous flow systems for bulk processing) with readily available equipment.

Another technique involves pre-treating waste prawn shells in hot glycerol, which also facilitates protein removal, likely through dehydration and temperature-induced fragmentation into low molecular weight, water-soluble fragments. These fragments are subsequently dissolved and washed away with water.[40] While the method demonstrated greater efficiency of deproteinization than that of the conventional chemical method, chitin characteristics such as extent of depolymerization and %DA were not reported.

Additionally, a fractionation method known as the hot water-carbonic acid (HOW-CA)[41] process has been developed to extract high-value chitin from crustacean shells. This method employs hot water for deproteinization and pressurized $CO_2$ for demineralization, achieving deproteinization and demineralization efficiencies exceeding 90% within just a few hours. However, deproteinization requires a temperature of ~180 °C, while demineralization is conducted at a pressure of 10 atm, which somewhat degrades the polymer, which is evident from the fact that chitin obtained from the HOW-CA process has a ~1.5-fold lower intrinsic viscosity molecular weight ($M\eta$ ~390 k) compared to that produced by conventional industrial methods (~570 k). There are also many efficient but relatively slow biological methods.[42]

The extraction of chitin is essential not only for its direct use but also as a sustainable feedstock for synthesizing valuable bio-based chemicals. Thus, chitin serves as a vital raw material to produce chitosan, glucosamine, *N*-acetylglucosamine, and various nitrogen-based fine chemicals.[43,44] Advancing eco-friendly and efficient extraction techniques is critical to harnessing the full potential of chitin, including from fungal sources.

For fungal biomass, conventional alkaline-based chitin isolation methods, such as sodium hydroxide pulping, effectively remove non-chitinous material by degradation and solubilization processes[47–62] but often lack selectivity, potentially degrading chitin and leading to lower Mw.[50,61] Additionally, the strong inter-allomorph interactions within the cell wall contribute to alkali-insolubility requiring intensive processing that can be both time-consuming and environmentally-taxing. Due to the structural similarity between glucans and chitin,[46] removing glucans is more challenging than removing other components. While NaOH is relatively inexpensive, its use produces alkaline waste that must be neutralized before disposal. Despite the availability of alternative solvents like ILs and DESs, widely demonstrated for chitin isolation from crustacean biomass,[35,63–69] their use has not been attempted for the isolation of fungal chitin.

This work assesses the impact of different isolation methods on the extraction and separation of chitin from white mushroom biomass (button mushroom, *Agaricus* bisporus), which provides a 'vegan' chitin option and addresses limit-

ations associated with crustacean-derived chitin. White mushrooms were chosen due to their relatively high chitin content (comparatively to other species), making them a suitable source for chitin extraction and analysis. Additionally, they are widely cultivated, commercially available year-round, and cost-effective, ensuring consistent and reproducible sample acquisition.[70] Their well-documented composition and previous use in chitin-related studies further support their selection as a model for this investigation.

To explore these alternatives for fungal sources, three different environmentally conscious methods were applied and compared with the conventional but unsustainable alkaline pulping. These methods include extraction using [$C_2$mim][OAc] (both thermal and microwave-assisted),[66] pulping using 1-butyl-3-methylimidazolium hydrogen sulfate ([$C_4$mim][$HSO_4$]),[71] and pulping with a DES made of lactic acid and choline chloride (LA : [Cho]Cl),[66,69] replicating procedures used for crustacean biomass. By comparing conventional and alternative approaches, we seek to determine whether these methods yield pure chitin or a chitin-glucan complex, an important distinction that influences its suitability for diverse applications. Additionally, understanding the yield and purity across various isolation techniques provides insights into their practical viability for industrial use. The effectiveness of each method, particularly regarding purity, is critical for potential applications in biotechnology and related fields. Ultimately, this research will clarify whether high-purity fungal chitin can be transformed into valuable C-based materials such as biodegradable scaffolds and fibers, thereby enhancing its commercial applicability. Moreover, optimizing isolation methods in a carbon-efficient manner aligns with sustainable biomass utilization, reducing waste and energy consumption in the process. This approach supports a circular economy, where fungal biomass can be maximized for C-based material production, further advancing environmental sustainability.

## Materials and methods

### Materials

Sodium hydroxide (NaOH) pellets were received from VWR (Radnor, PA). The ionic liquids, 1-ethyl-3-methylimidazolium acetate ([$C_2$mim][OAc]) and 1-butyl-3-methylimidazolium hydrogen sulfate ([$C_4$mim][$HSO_4$]) were obtained from ProIonic Gmbh (Graz, Austria). Lactic acid (LA) and choline chloride ([Cho]Cl) were received from Sigma-Aldrich (St Louis, MO, USA). Chitin (from shrimp shells) and chitosan samples (30.0% DA) were obtained from Sigma Aldrich (St Louis, MO, USA). MilliQ water (DI water) purified using a Millipore Milli-Q lab water system (Burlington, MA, USA) with a conductivity of 4.2 MΩ cm$^{-1}$ was used for chitin precipitation and washing. Lactic acid and [Cho]Cl DES (LA : [Cho]Cl = 2 : 1 mol mol$^{-1}$) was prepared by placing the beaker with both components (LA: 18 g, [Cho]Cl: 14 g) inside a oven at 105 °C (Fisher Scientific, Pittsburgh, PA, USA) until components were fully melted (~1 h).

Whole white mushrooms donated by Chitozan Health, LLC (Avondale, PA) were utilized for the process. The biomass was dried in an oven at 50 °C overnight and then ground to <125 μm, using a CGoldenwall grinder (Jiangyin City, China). The ground dry biomass was stored in tightly closed plastic centrifuge tubes.

## Isolation of chitin from white mushroom species

**Pulping with 1 M NaOH.** This benchmark method, pulping fungal biomass with NaOH, was adapted from a previous report.[72] Briefly, 0.5 g biomass was placed into a 25 mL round-bottom flask, equipped with a condenser and a stir bar, followed by the addition of 15 mL 1 M NaOH solution. The suspension was heated to 80 °C, using an IKA hot plate (Wilmington, NC, USA) equipped with a heating aluminum block (DrySyn MULTI-E, Asynt Ltd, Cambridgeshire, UK) and stirred at 700 rpm for 2 h. After 2 h, the suspension was allowed to cool to room temperature, transferred into 15 mL centrifuge tubes, and centrifuged (StonyLab, Nesconset, NY, USA) for 15 min at 5000 rpm. The liquid was decanted, fresh MilliQ water was added, and the suspension was centrifuged again. Water washings were repeated 10 more times until the pH of the supernatant reached 6.5. The samples were then placed onto Petri dishes, dried in the oven overnight, weighed to determine the yield, and analyzed for purity.

**Thermal extraction using [C$_2$mim][OAc].** This method was adapted from previous report for extraction of chitin from crustacean biomass.[66] Briefly, 5.0 g of biomass was added to a 100 mL round-bottom flask equipped with a stir bar. Then, 50 g of [C$_2$mim][OAc] was added to the flask. The suspension was stirred at 700 rpm and heated to 100 °C on an IKA hot plate using a DrySyn MULTI-E aluminum heating block for 48 h. After 48 h, the mixture was cooled to room temperature and transferred into 15 mL centrifuge tubes. The suspension was then centrifuged (at 5000 rpm for 15 min, to separate the liquid and solid phases). The supernatant, containing IL-dissolved product, was decanted, then poured into water to precipitate the extracted compound(s). The precipitate was washed 10 times with fresh DI water, with centrifugation and decantation performed after each wash, until the suspension's pH reached 6.5. The washed precipitate was transferred to Petri dishes, dried overnight in an oven, and subsequently weighed to determine yield. The samples were then analyzed to assess purity.

**Microwave-assisted extraction using [C$_2$mim][OAc].** This method was adapted from previous report for extraction of chitin from crustacean biomass.[66] Briefly, 0.5 g biomass was placed into a 25 mL Erlenmeyer flask, equipped with a glass rod and a stir bar, followed by the addition of 9.97 g [C$_2$mim][OAc]. The suspension was stirred with a glass rod, placed inside a microwave oven, and heated for 2 and 5 min, with 2-sec pulses. After completion of the heating time, the suspension was transferred to 15 mL centrifuge tubes and centrifuged for 15 min at 5000 rpm. The undissolved solid precipitate (precipitate 1) was then washed with DI water (16 mL × 10 times) until the pH of the water reached 6.5. The precipitate

was placed on Petri dishes and dried in the oven, weighed to determine the yield, and analyzed.

**Pulping using [C$_4$mim][HSO$_4$].** This method was adapted from previous report for extraction of chitin from crustacean biomass.[73] Briefly, 48.5 g [C$_4$mim][HSO$_4$] was heated in a flask until melted, followed by the addition of 1.5 g white mushroom biomass. The suspension was kept inside the oven at 50 °C for 24 h. After 24 h, 16.7 mL DI water was added to the flask, and the suspension was refluxed at 100 °C for 24 h with stirring on a hot plate. After 24 h, the suspension was transferred to 15 mL centrifuge tubes, centrifuged, and the precipitate was washed 15 times with DI water up to a pH of 6.5. After that, the suspension was frozen at −20 °C and lyophilized using the following conditions: −90 °C, 0.06 mbar, 48 h (Labconco FreeZOne Plus Cascade Benchtop Freeze Dryer System, Kansas City, MO, USA).

**Pulping using 2 : 1 lactic acid : [Cho]Cl.** This method was adapted from previous report for pulping of chitin from crustacean biomass.[74] Briefly, 0.5 g biomass was placed into a 25 mL round-bottom flask, equipped with a condenser and a stir bar, followed by the addition of 4.5 g lactic acid : [Cho]Cl. The suspension was heated to 100 °C using an IKA hot plate and stirred at 700 rpm for 3 h. After 3 h, the suspension was allowed to cool to room temperature, transferred to 15 mL centrifuge tubes, and centrifuged for 15 min at 5000 rpm to isolate the precipitate. The precipitate was repeatedly washed with DI water (15 mL × 10 times) until the pH of the water reached 6.5. The precipitates were then placed on Petri dishes, dried in an oven, weighed to determine the yield, and analyzed.

## Preparation of fibers

0.25 g isolated chitin from white mushrooms was added to a flask containing 9.75 g [C$_2$mim][OAc]. The flask was sealed with a septum pinched with a needle and placed into a heating block (100 °C, 700 rpm), and heated with magnetic stirring until complete dissolution of the chitin (~24 h). The flask was then removed from the heating block, the stir bar removed, and the solution was transferred to centrifugation tubes. The solution was centrifuged for 15 min at 5000 rpm to separate any undissolved residue. After centrifugation, the solution was warmed in the oven (75 °C) for about 35 min to reduce its viscosity and degas, and then transferred to a 12 mL plastic syringe of 14 mm diameter, with a nozzle tip of 1.5 mm diameter. The syringe was then placed in a syringe pump (New Era Pump Systems, Inc. NE-1010, Farmingdale, NY, USA) so that the syringe tip was located *ca.* 1–2 mm above the water surface. Fibers were extruded into the water bath (*ca.* 1.5 L) at the extrusion rate of 1.6 mL min$^{-1}$. Fibers were collected on an empty centrifuge tube, washed with DI water 10 times, and dried for further characterization.

## Characterization techniques

**Attenuated total reflectance (ATR) Fourier-transform infrared spectroscopy (FTIR).** An ATR FTIR Spectrum-400 (PerkinElmer, Waltham, MA, USA) was used to characterize the

isolated materials. The samples were conditioned in a controlled environment at 21 ± 1 °C and 65 ± 2% relative humidity before being analyzed on a chemically inert Zn–Se diamond crystal stage. The spectral resolution was set at 4 cm$^{-1}$, and a total of 64 scans which include the spectral range from 650 to 4000 cm$^{-1}$ were carried out. The data were evaluated using OPUS Bruker software version 7.1 (Bruker Optics, Billerica, MA, USA), compatible with the PerkinElmer instrument.

**Solid-state $^{13}$C multi cross-polarization magic angle spinning nuclear magnetic resonance (SS $^{13}$C multiCP-MAS NMR) spectroscopy.** SS $^{13}$C multiCP-MAS NMR spectra were acquired on an Agilent DD2 600 MHz NMR spectrometer (Santa Clara, CA), configured for biomolecular solid-state NMR (SSNMR) experiments. It is a three-channel instrument equipped with a custom HCN Balun Probe, an HCN BioMAS probe, and an HXY fastMAS probe. The instrument was controlled by a Dell workstation running RedHat Linus and the VNMRJ 3.2 NMR software. The chitin was center packed into FastMAS Agilent rotor and spun at 8 kHz. The pulse sequences and basic CP parameters were based on those reported.[12] A total of 2500 scans were acquired for each sample. The data were processed using MestreNova 15.1 (Mestrelab Research, San Diego, CA, USA)

**Determination of degree of acetylation (%DA).** In the SS $^{13}$C multiCP-MAS NMR spectrum of chitin, there are specific peaks that correspond to the carbonyl carbon (C=O) of the acetyl group, at around 170–175 ppm, and the carbon atoms of the glucosamine ring (C1–C5) at around 50–110 ppm. The %DA was calculated (eqn (1)) using the area (integral value) of the peak corresponding to the C=O and the sum of the peaks from the glucosamine ring:

$$\%DA = 100 \times \frac{I_{CH3}}{\frac{1}{5}\sum I_{C1,C2,C3,C4,C5}} \quad (1)$$

where $I$ is the integration value.

**Purity evaluation.** The purity was calculated according to eqn (2):

$$\%Purity = 100 \times \frac{\sum I_{target\ compound\ (chitin)}}{\sum total\ integration} \quad (2)$$

where $I_{target\ compound}$ refers to the integrated area corresponding to the target compound's peaks (*e.g.*, chitin's characteristic peaks), and total integration refers to the integrated area corresponding to peaks from both chitin and impurities.

**Thermogravimetric analysis (TGA).** A TG/DTA Simultaneous measuring instrument (Shimadzu DTG-60H, Kyoto, Japan) was used to analyze the thermal stability of the isolated materials. Before analysis, the samples were maintained in regulated conditions at 21 ± 1 °C and 65 ± 2% relative humidity. Nitrogen was pumped in at a rate of 100 mL min$^{-1}$ to keep the environment inert. The temperature range for the thermal analysis was 25 to 600 °C, with a heating rate of 5 °C min$^{-1}$. The data obtained from the analysis was interpreted by the instrument operating software (Shimadzu, Kyoto, Japan). To obtain a DTG

curve, the mass change data from TGA was numerically differentiated using Origin 2018 (OriginLab Corporation, Northampton, MA, USA), and the resulting values were plotted against temperature, with peaks indicating the temperatures where the rate of mass change was highest. This analysis was performed using Origin 2018 (OriginLab Corporation, Northampton, MA).

**Viscosity measurements.** The viscosity of the isolated chitinous materials was measured using a viscometer (PAC Viscolab 4000, PAC, Houston, TX, USA). The samples included high molecular weight crustacean chitin (prepared as described in ref. 66), chitin extracted from white mushrooms using thermal dissolution in [C$_2$mim][OAc] (Wh/Chitin$_{[C_2mim][OAc]}$), and chitin from white mushrooms purified by NaOH treatment for 24 h (Wh/Chitin$_{NaOH-24}$). Each sample was dissolved in [C$_2$mim][OAc] at a concentration of 2.5 wt% and maintained at 100 °C for 24 h. After 24 h, the solution was placed into the centrifuge for 15 min to separate any (minor) undissolved residue. The remaining solution was run in a viscometer to obtain the viscosity values (piston 0.2 to 10 000 cP) at different temperatures from 40 to 100 °C. The data obtained were plotted and analyzed in Sigma Plot, SYSTAT, Version 11.00 (Santa Clara, CA, USA).

**Estimation of crystallinity.** A powder X-ray diffractometer (HD 2711N, Rigaku, Tokyo, Japan) with Ni-filtered Cu Kα radiation and $\lambda$ = 1.542 Å, at 44 mA and 40 kV, was used to determine the crystallinity of the isolated materials from the mushroom biomass. Diffractograms were obtained over the 5 to 50°, at a scanning rate of 1° min$^{-1}$. Origin software was used to find and subtract the baseline in the spectrum, detect the peaks, and calculate the peak areas. The crystallinity of the isolated material was calculated using the obtained area from multiple peak fitting following eqn (3):

$$\%CrI = \frac{\sum area\ of\ cryst.\ peaks}{\sum area\ (cryst.\ peaks + amorph.\ scattering)} \times 100 \quad (3)$$

where CrI (%) is a crystallinity index.

**Crystallite size determination.** The Scherrer equation (eqn (4)) was used to calculate the crystallite size:[75,76]

$$\beta = (k \times \lambda)/(L \times \cos(\theta)) \quad (4)$$

where $\beta$ is the crystallite size that is perpendicular to the lattice plane represented by (020) and (110) peaks, $k$ represents the Scherrer constant for a given crystal shape ($k$ = 0.91), $\lambda$ represents the wavelength of the incident X-rays (1.54 Å), $L$ represents the width of the peak at half of its maximum in radians (FWHM), and $\theta$ is the position of the peak (half of the plotted $2\theta$ value).

**Scanning electron microscopy (SEM).** The analysis of the morphology of prepared fibers was performed using a field emission scanning electron microscope (FE-SEM, Hitachi S-4700, Tokyo, Japan). The measurement was conducted in the secondary electron imaging mode at an accelerating voltage of 2 kV, beam current of 10 Å, and a working distance of 12 mm.

**Tensile testing.** The diameter of the specimens was measured following ASTM D3822-07 Standard Test Method criteria.[77] The tensile measurements were recorded using the Multi-Test 2.5-dV(u) Test System (Mecmesin, Slinfold, West Sussex, UK). The load, gauge length, and the instrument's speed were set at 10 N, 20 mm, and $30 \pm 10$ mm min$^{-1}$, respectively. All the tensile measurement data were examined and computed using the VectorProTM 431-955-03 software (version 8.3.0.0, Slinfold, West Sussex, UK). The data obtained were plotted in Sigma Plot, SYSTAT, Version 11.00 (Santa Clara, CA, USA).

# Results and discussion

Dried and ground biomass from white mushroom (button mushroom, *Agaricus* bisporus) was subjected to four different treatments. The first treatment was traditional pulping using NaOH (Fig. S1, ESI†). The reaction parameters for the NaOH pulping method were selected based on a literature review of similar studies for mushrooms.[47–62] For this method, the temperature was kept constant at 80 °C, and two different reaction times, *i.e.*, 2 and 24 h, were tested to assess how extended reaction times might affect the deacetylation process. After the reaction, the crude product was isolated through centrifugation, followed by washing and drying steps. The final treated materials were labeled according to the duration of the treatment, *i.e.*, Wh/Chitin$_{NaOH-2}$ and Wh/Chitin$_{NaOH-24}$, respectively.

For the second method of chitin isolation, we employed extraction using [C$_2$mim][OAc]. The choice between thermal and microwave heating methods can have a significant impact on the efficiency of the isolation method and the quality of the isolate. Typically, thermal heating involves using conventional heat sources resulting in a gradual, relatively slow, steady heating rate. Microwave heating directly excites polar [C$_2$mim][OAc] molecules resulting in rapid, volumetric heating from within the biomass, making it significantly faster than thermal methods. However, this could lead to a less pure compound especially if the biomass contains proteins that interact strongly with microwaves,[78] sometimes requiring further purification steps. Regardless of the heating method, [C$_2$mim][OAc] dissolves biopolymer from the biomass by disrupting the hydrogen bonds within the polymer chain.[79] The biomass and IL were heated in a microwave oven in 2-sec pulses for 2 and 5 min (Fig. S2, ESI†). Since no significant differences were observed between the two durations, the results and discussion will focus on the 2 min protocol. The material obtained was labeled Wh/Chitin$_{[C_2mim][OAc]\ Microwave}$. Traditional heating was also evaluated for the same IL (Fig. S3, ESI†), *i.e.*, heating the suspension of biomass in IL in an oil bath at 100 °C for 48 h. The isolated product was denoted as Wh/Chitin$_{[C_2mim][OAc]\ Thermal}$.

The IL [C$_4$mim][HSO$_4$] was used in the third isolation strategy (Fig. S4, ESI†), where the basic and acidic functionalities needed for deproteinization and demineralization were combined in a single IL. The process consisted of two steps: the

pretreatment when the biomass was added to the IL and allowed to rest for 24 h, and hydrolysis, when water was added to the mixture, and the suspension was left at reflux for another 24 h before centrifugation and washing. After this, the residue was collected, washed, the suspension frozen, and the isolate was dried by lyophilization. The material obtained from this method was labeled Wh/Chitin$_{[C_4mim][HSO_4]}$.

In the fourth method for chitin isolation, a DES, composed of lactic acid and [Cho]Cl (2 : 1 mol : mol), was used. Biomass was mixed with the DES and heated at a constant temperature of 100 °C for 3 h. After the reaction, the suspensions were centrifuged, washed, and dried. The material isolated from this method was labeled as Wh/Chitin$_{DES}$.

### Characterization of the materials isolated

**Appearance and yields.** The initial appearance of the isolates from the mushroom biomass (which itself was of medium-brown color) varied in shades of black (Table 1 and Fig. S5, ESI†). After treatment with NaOH (Fig. S1, ESI†), [C$_2$mim][OAc] (Fig. S2 and S3, ESI†), [C$_4$mim][HSO$_4$] (Fig. S4, ESI†), or DES (no picture provided), the isolated materials turned black from the initially brown-colored white mushroom biomass (Fig. S5, ESI†). After treatment with [C$_2$mim][OAc], the isolated materials were also shiny (Fig. S5, ESI†).

The crude yields of isolates, which may include impurities such as alkali-insoluble glucans (*i.e.*, β-1,3 and 1,6-glucans which possess β-1,4-linkages to chitin[26,46]) and/or glycoproteins present in white mushroom biomass, were then calculated (Table 1). The ideal yield was expected to fall within the 7–12% range, based on previous reports for isolates from white mushrooms. For instance, Hassainia *et al.* reported a chitin yield of 7.4% from white mushroom stipes,[80] while Singh and Dutta documented a crude yield of 12% from white mushrooms.[62] In our case, when NaOH, DES, and the 'pulping' [C$_4$mim][HSO$_4$] were used, the goal was to dissolve impurities such as glucans and proteins. However, not all impurities were removed; some remain associated with the chitin. In contrast, with 'extracting' [C$_2$mim][OAc], the aim was to dissolve chitin itself, but some glucans and/or proteins also dissolved in the process. Hence, high crude yields suggest that the crude isolates could contain a significant proportion of other biomass components, such as glucans and/or proteins, however, at this stage, any assessment of purity would be speculative. Therefore, we proceeded with detailed purity ana-

**Table 1** Yield and appearance of isolated materials from different treatments

| Samples | Appearance | Crude yield, % |
|---|---|---|
| Wh/Chitin$_{NaOH-2}$ | Faded black | $27.1 \pm 8.0$ |
| Wh/Chitin$_{NaOH-24}$ | Faded black | $10.1 \pm 0.9$ |
| Wh/Chitin$_{[C_2mim][OAc]\ Thermal}$ | Faded black | $9.6 \pm 3.1$ |
| Wh/Chitin$_{[C_2mim][OAc]\ Microwave}$ | Shiny faded black | $14.6 \pm 1.6$ |
| Wh/Chitin$_{[C_4mim][HSO_4]}$ | Faded black | $23.8 \pm 0.4$ |
| Wh/Chitin$_{DES}$ | Faded black | $30.6 \pm 1.4$ |

lysis with FTIR, ^{13}C multiCP-MAS NMR, and TGA as described below.

**Purity of chitinous isolates.** ATR-FTIR, solid-state NMR, and thermogravimetric analysis (TGA) were used to quantify impurities in the isolated chitinous fractions. The fractions were compared with standard references for chitin and chitosan, as well as the original biomass.

**FTIR characterization.** Both glucans and chitin are polysaccharides and share similar structural features, such as a backbone of glucose units, C–O stretching, and O–H stretching bands; such similarity complicates the interpretation of their FTIR spectra. While glucans generally do not contain N–H bonds, as they are primarily composed of glucose units linked by glycosidic bonds, glycoproteins such as galactosaminogalactan and cell wall structural proteins may produce N–H stretching observed in the FTIR spectra. The overlapping absorption bands in the FTIR spectra can make it challenging to differentiate between those associated with glucans and glycoproteins, and those attributed to chitin. Several different types of glucans in the samples make it even harder to identify specific bands unique to glucans or chitin.

A comparison between the FTIR spectra of the biomass, material isolates, and commercial chitin (Fig. 2) displays notable differences in the regions corresponding to O–H stretching at ~3400 cm$^{-1}$, N–H stretching at ~3100 and 3260 cm$^{-1}$ and C–H stretches of CH, CH$_2$, and CH$_3$ groups at 3000–2800 cm$^{-1}$ (Fig. 1 bottom and Fig. S6† (full spectrum, ESI†)).[81] The biomass exhibits significantly higher intensity peaks associated with O–H stretching compared to all isolated products, indicating the presence of both chitin and glucan O–H groups.[81,82]

In this region, the spectra profiles of all isolates resemble that of commercial chitin and not biomass, except Wh/Chitin$_{DES}$ which displays the highest intensity O–H stretch among all samples, likely due to retaining a higher fraction of glucans and other hydroxyl-containing carbohydrates, contributing to the increased intensity of the O–H stretching region. However, we also noted that all samples -except for Wh/ChitinNaOH-24 -exhibited higher O–H band intensities compared to commercial crustacean chitin. These variations could stem from the differences in the isolation methods. Specifically, commercial chitin and NaOH-24-treated chitin exhibit high crystallinity, with well-ordered structures and extensive O–H-associated hydrogen bonding. In contrast, IL- and DES-treated chitins are more amorphous, resulting in less hydrogen bonding and an increased number of available O–H groups, which could contribute to the observed spectral differences.

To further support the presence of chitin in all isolates, additional functional peaks closely resembling the spectrum of commercial chitin were identified (Fig. 1 and Fig. S7, ESI†): CH$_2$ wagging (amide III) at 1308 cm$^{-1}$, C–O–C asymmetrical stretch occurs at 1155 cm$^{-1}$, the C$_6$–OH stretching at 1021 cm$^{-1}$, and the C$_3$–OH stretch at 1070 cm$^{-1}$, and β-glycosidic bond at 895 cm$^{-1}$, present in all isolates (Fig. 1 bottom and Fig. S6, ESI†).
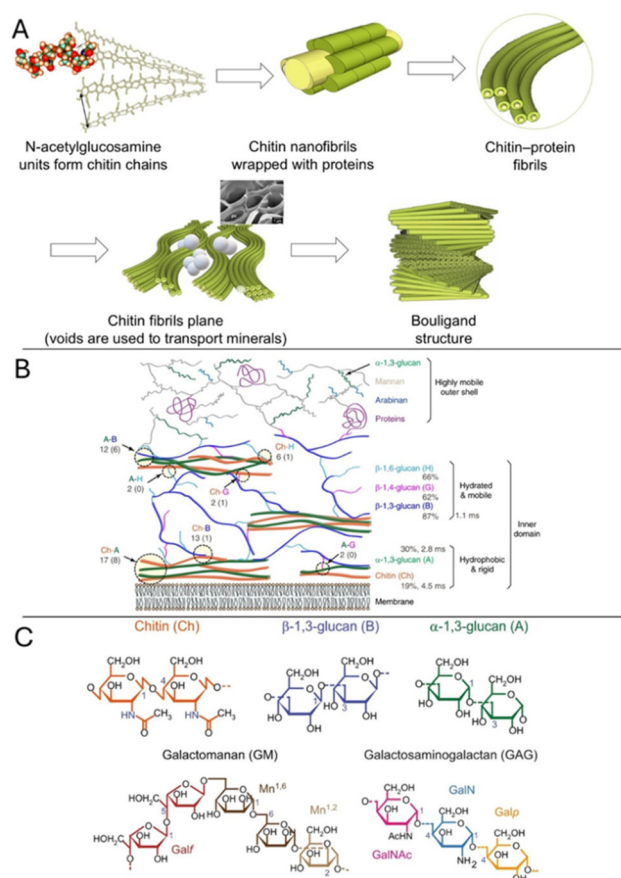


**Fig. 1** Differences between the composition and structural features of crustacean cuticle and fungal cell walls. (A) Composition of crustacean cuticle (adapted from ref. 45, Copyright 2011 Elsevier); (B) representation of the components of fungal cell wall (adapted from ref. 46, Copyright 2021 Springer Nature); (C) fungal cell wall components (adapted from ref. 46, Copyright 2021 Springer Nature).

The most noticeable spectral difference among the samples was observed in the amide region (Fig. 2, top). The characteristic FTIR peaks of commercial α-chitin are the amide I and amide II bands. In a typical α-chitin spectrum, the amide I band is split into two components at 1654 cm$^{-1}$ and 1630 cm$^{-1}$ due to differences in hydrogen bonding.[82] The 1654 cm$^{-1}$ band corresponds to the C=O stretching mode hydrogen-bonded to the N–H of a neighboring intra-sheet chain (i.e., C=O···HN–) while the 1630 cm$^{-1}$ band represents a specific stretching mode of C=O hydrogen bonded to HO– within the same chain (i.e., O=C···HOCH$_2$–). The amide II band (~1550 cm$^{-1}$) in chitin is associated with N–H bending and C–N stretching vibrations of amide.[83–85]

Chitosan typically exhibits O–H, N–H, and C–H stretching vibrations along with amide I and II bands. However, in chitosan, the amide I band primarily originates from the C=O stretching vibrations of residual acetyl groups due to incomplete deacetylation of chitin. As expected, its intensity decreases with decreasing %DA, reflecting a reduction in acetyl (–CONHCH$_3$) groups. Similarly, the amide II band,
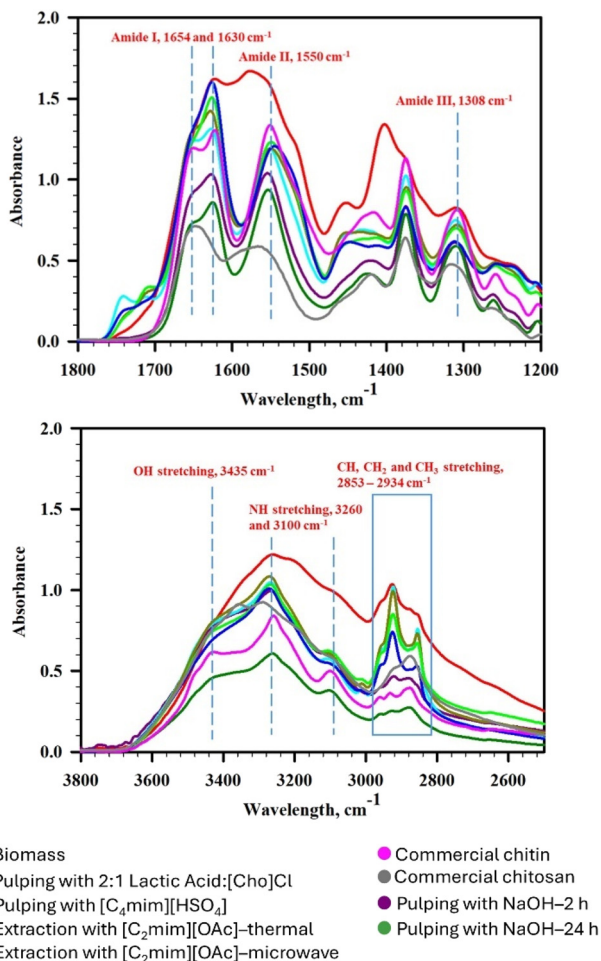
**Fig. 2** FTIR spectra (top: region 1800–1200 cm$^{-1}$, bottom: region 3800–2500 cm$^{-1}$) of biomass (red), commercial chitin (pink), commercial chitosan (grey) and isolated materials by four different methods: pulping with NaOH-2 h (purple), pulping with NaOH-24 h (dark green), extraction with [C$_2$mim][OAc]–microwave (cyan), extraction with [C$_2$mim][OAc]–thermal (olive), pulping with [C$_4$mim][HSO$_4$] (light green), and pulping with 2 : 1 lactic acid : [Cho]Cl (blue).

appear more intense than the amide I band, likely due to residual proteins,[28] whose C=O···H–N bonds contribute to the same spectral region. In Wh/Chitin$_{DES}$, the intensity of these peaks is nearly as intense as those in raw biomass, suggesting that the DES treatment retains more residual biomass components than other methods, producing isolates that closely resemble the original material.

To estimate the extent of deacetylation (later quantified precisely with $^{13}$C NMR spectroscopy), we analyzed the splitting of the C=O stretch, the relative intensities of the amide I and amide II bands, and the presence or absence of the 1598 cm$^{-1}$ peak to differentiate chitin from chitosan. The absence of this peak in the FTIR spectra of the chitin isolates suggests a relatively high %DA across all samples, implying that the chitin has not undergone extensive deacetylation and retains its acetylated structure. Additionally, the spectra of the isolated products were compared with that of chitosan (Fig. 2, top, grey plot) to further highlight these differences.

**SS $^{13}$C multiCP-MAS NMR.** To further study the purity of isolated solid materials, SS $^{13}$C multiCP-MAS NMR was used as previously reported (Fig. 3).[12] This method allows for the quantification of chitin content (and therefore purity) in extracted chitin samples in a quick, clean, non-destructive manner. The results were shown to agree with those obtained from the method of Black and Schwartz.[87] Here, the use of multiCP enhances the signal of low-abundance nuclei such as $^{13}$C by transferring polarization from more abundant nuclei like $^{1}$H, whereas MAS (~54.7° relative to the external magnetic field) helps achieve high-resolution spectra for solid samples. The analysis allows not only identifying key carbon peaks (C1–C6, carbonyl C=O, and CH$_3$ carbon) and comparison with reference spectra, but also quantifies the relative intensities of the peaks[88] by integrating the signals, as the area under each

associated with N–H bending and C–N stretching vibrations, confirms the presence of residual amide groups from chitin and decreases accordingly upon deacetylation. The intensities of both peaks in chitosan are significantly lower than in chitin and vary based on the degree of deacetylation (Fig. 2, top, grey pattern). Another distinguishing feature of chitosan is a peak at 1590–1598 cm$^{-1}$, corresponding to the bending vibration of the –NH$_2$ group.

The FTIR spectra reveal that amide I band splitting is evident in Wh/Chitin$_{NaOH-24}$ and Wh/Chitin$_{[C_2mim][OAc]}$, with sharp and resolved peaks, in contrast to untreated biomass (Fig. 2 top). Notably, the intensities of the amide I and amide II bands are comparable. The relative intensities between these bands in these treatments closely resemble that in commercial chitin, suggesting effective removal of extraneous proteinaceous matter.[82,86] In contrast, Wh/Chitin$_{[C_4mim][HSO_4]}$ and Wh/Chitin$_{DES}$ isolates exhibit unresolved amide I peaks, which
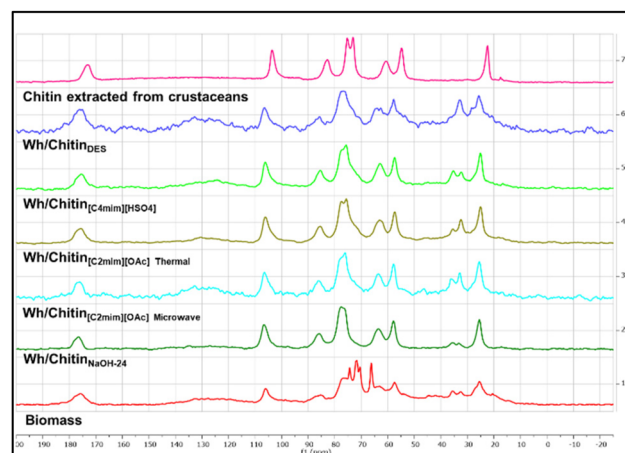


**Fig. 3** Comparison of solid-state $^{13}$C multiCP-MAS NMR spectra of biomass (red) and isolated materials from (olive) pulping with NaOH-24 h, (green) extraction with [C$_2$mim][OAc]–microwave, (cyan) extraction with [C$_2$mim][OAc]–thermal, (blue) pulping with [C$_4$mim][HSO$_4$], (purple) pulping with 2 : 1 lactic acid : [Cho]Cl, (pink) chitin extracted from crustacean biomass using [C$_2$mim][OAc].

peak becomes directly proportional to the number of carbon atoms that contribute to that peak. In addition, if the chitin has been partially deacetylated, a reduction in the intensity of the carbonyl peak (~170–175 ppm) or methyl carbon (20–25 ppm) in respect to C1–C6 allows to directly calculate %DA.

The $^{13}C$ multi-MAS NMR spectrum for Wh/Chitin$_{NaOH-24}$ (Fig. S10, ESI†) reveals chemical shifts at $\delta$ 176.5, 106.5, 86.0, 77.6, 76.2, 63.6, 57.8, and 25.5 ppm, corresponding to the C=O carbon, C1, C4, C5, C3, C6, C2, and the CH$_3$ carbon, respectively. These signals confirm the presence of chitin and indicate that the treatment successfully isolated chitin from the biomass. The partial resolution of peaks for the C3 and C5 atoms suggests that the chitin is in its α-crystalline form.[89,90] The spectrum also reveals impurities, with additional peaks other than chitin. These peaks, however, were partially obscured by the chitin spectrum, due to overlapping in their chemical shifts. The peaks not overlapping with chitin were found primarily in regions 120–140 and 20–40 ppm, arising from aromatic and aliphatic resonances of residual protein contaminations, respectively.[12,91] Importantly, no glucans were detected, confirming their effective removal during the 24-hour NaOH treatment. To further support these findings, we included an image from a published study where chitin and glucan signals are well-resolved, enabling clearer differentiation. Additionally, we provided a table in the ESI† detailing the glucan peaks for reference. The degree of acetylation (%DA), calculated from the $^{13}C$ NMR spectrum, was 72%, and the purity of the material, based on the integration of the $^{13}C$ multiCP-MAS NMR spectrum, was approximately 77%. The estimated amount of chitin in the Wh/Chitin$_{NaOH-24}$ sample was calculated by multiplying the crude yield by the purity (Table 2) and was found to be 7.7%, consistent with the expected 7–12% range.[62,80]

The SS $^{13}C$ multiCP-MAS NMR spectrum of Wh/Chitin$_{[C_2mim][OAc]\ Thermal}$ (Fig. S11, ESI†) closely resembled that of Wh/Chitin$_{NaOH-24}$, with peaks consistent with the expected chitin structure. Both samples exhibited impurities at 20–40 ppm and 120–140 ppm, indicative of protein contamination. The calculated purity from $^{13}C$ multiCP-MAS spectral integration was 77%, matching that of the NaOH-treated sample. Considering this level of purity, the estimated chitin content in Wh/Chitin$_{[C_2mim][OAc]\ Thermal}$ was 7.4% (Table 2).

The %DA, calculated from the $^{13}C$ NMR, was 75%, slightly higher than the %DA for Wh/Chitin$_{NaOH-24}$. Overall, both the NaOH and [C$_2$mim][OAc]-thermal treatments produced chitin isolates with similar purity, type of residual contaminants (i.e. proteins but no glucans), and %DA.

In contrast, the SS 13C multiCP-MAS NMR spectrum of the microwave-irradiated Wh/Chitin$_{[C_2mim][OAc]}$ sample (Fig. S12, ESI†) exhibited more pronounced protein peaks[12] (at 20–40 ppm and 120–140 ppm) compared to the thermally treated sample. Additional impurities were observed in the 90–100 ppm and 40–60 ppm regions, likely unrelated to glucans or proteins in the biomass, as indicated by comparisons with the biomass spectrum. The emergence of new peaks in the microwave-irradiated sample, compared to the thermally heated sample, could be due to faster and less controlled extraction conditions, potentially accelerating carbohydrate degradation. The purity of material calculated from integration of $^{13}C$ multiCP-MAS spectra was 63%, and the estimated amount of chitin in the Wh/Chitin$_{[C_2mim][OAc]\ Microwave}$ sample was 8.8% (Table 2). The %DA of microwave-irradiated Wh/Chitin$_{[C_2mim][OAc]}$ sample calculated by $^{13}C$ NMR was 71%.

The $^{13}C$ multiCP-MAS NMR spectrum of Wh/Chitin$_{[C_4mim][HSO_4]}$ (Fig. S13, ESI†) closely resembles that of Wh/Chitin$_{[C_2mim][OAc]\ Microwave}$, with similar peak positions and overall spectral features. Both spectra indicate the presence of the same types of impurities; however, the Wh/Chitin$_{[C_4mim][HSO_4]}$ sample shows a significantly higher level of impurities. The differences in the solubility of proteins in the two ILs might explain the variation in purity. The strong acidity of [C$_4$mim][HSO$_4$] could hydrolyze protein structures, causing them to co-extract with the chitin, increasing the level of contamination. The %DA and purity calculated from the $^{13}C$ spectra of Wh/Chitin$_{[C_4mim][HSO_4]}$ were 70% and 40%, respectively, with an estimated amount of chitin in the sample of 9.5% (Table 2).

The spectrum of Wh/Chitin$_{DES}$ displays strong similarities to the pretty complex spectrum of the original biomass (Fig. S14, ESI†), particularly in terms of peak positions and overall spectral pattern. The peak broadening around 100–103 ppm (C1 region) suggests the presence of both chitin and glucan, as both materials produce signals in this range. Similarly, broader peaks in the 60–85 ppm region, where the C4, C5, and C6 carbons of both polymers overlap, might imply

**Table 2** Characterization summary of the products isolated from white mushroom biomass

| Samples | Crude yield, % | Purity, % | Amount of chitin in biomass, %[a] | CrI, % | Crystallite size 020 plane, nm | Crystallite size 110 plane, nm | %DA | DTG$_{max}$, °C |
|---|---|---|---|---|---|---|---|---|
| Wh/Chitin$_{NaOH-2}$ | 27.1 ± 8.0 | ND | ND[b] | 80.3 | 4.1 | 3.9 | 72 | 324.1 |
| Wh/Chitin$_{NaOH-24}$ | 10.1 ± 0.9 | 77.0 | 7.7 | 84.8 | 3.9 | 3.0 | 72 | 348.6 |
| Wh/Chitin$_{[C_2mim][OAc]\ Thermal}$ | 09.6 ± 3.1 | 77.0 | 7.4 | 64.5 | 4.8 | 3.8 | 75 | 343.9 |
| Wh/Chitin$_{[C_2mim][OAc]\ Microwave}$ | 14.6 ± 1.6 | 63.0 | 8.8 | 66.1 | 3.8 | 3.5 | 71 | 322.6 |
| Wh/Chitin$_{[C_4mim][HSO_4]}$ | 23.8 ± 0.4 | 40.0 | 9.5 | 63.3 | 4.9 | 2.7 | 70 | 309.2 |
| Wh/Chitin$_{DES}$ | 30.6 ± 1.4 | 29.8 | 9.1 | 63.0 | 3.8 | 4.2 | ND | 300.9 |

$^a$ Calculated by multiplying crude yield and purity. $^b$ ND – not determined.

combined signals from both chitin and glucan. In particular, the peaks in the $^{13}$C NMR spectra of Wh/Chitin$_{DES}$ within the C1 region (100–103 ppm) and C4–C6 region (60–85 ppm) are noticeably broader than those in a pure chitin spectrum (Fig. S8, ESI†), likely indicating glucan contamination. The %DA was not calculated from the $^{13}$C spectra of Wh/Chitin$_{DES}$ due to the material's low purity, which was estimated to be around 30%, with an estimated amount of chitin in the Wh/Chitin$_{DES}$ sample of 9.1%.

These results well explain the high crude yield of isolates, obtained from white mushroom biomass after a 3 h treatment with DES (30.6 ± 1.4%), 2 h treatment with NaOH (27.1 ± 8.0%), as well as the treatment with [C$_4$mim][HSO$_4$] (23.8 ± 0.4%). Overall, the NMR study confirms that these isolates contain a substantial amount of biomass components other than chitin itself. NMR also confirms, that, by contrast, microwave-assisted extraction with [C$_2$mim][OAc] which yielded 14.6 ± 1.6%, just slightly exceeds the expected purity range proving that the isolate contains impurities, but not in significant amounts. Extending the NaOH treatment to 24 h resulted in a significant decrease in yield (10.1 ± 0.9%) when compared to 2 h treatment. Such longer treatment likely removed glucans and proteins, which results in a lower yield, but significantly purer polymer. Thermal extraction of white mushroom biomass using [C$_2$mim][OAc] produced an isolate of 9.6 ± 3.1%. This falls within the expected purity range, confirming the conclusion from NMR that the product is relatively pure. Based on the determined purity levels, the amount of chitin in biomass was found to be between 7.7 and 9.6%, within the expected 7–12% range.

Different chitin isolation methods affected protein removal efficiency. The DES treatment was mostly ineffective, resulting in the retention of both glucans and proteins within the sample. Pulping with the IL [C$_4$mim][HSO$_4$] was less efficient than NaOH treatment, whereas the IL [C$_2$mim][OAc] demonstrated greater extraction efficiency compared to both DES and [C$_4$mim][HSO$_4$], yet it was still less effective than NaOH. NaOH, as anticipated, demonstrated a highly effective deproteinization by disrupting hydrogen bonds and ionic forces within proteins, causing them to unfold and lose their native structure. At elevated pH, NaOH facilitates the hydrolysis of amide bonds, breaking proteins into smaller peptides or free amino acids, which were easily removed through washing.

The mildly basic ionic liquid [C$_2$mim][OAc] (pH ~8–10) has been shown to dissolve proteins by disrupting hydrogen bonds, breaking down secondary structures (α-helices and β-sheets), and catalyzing peptide bond hydrolysis, leading to protein solubilization. These properties have been applied in the preparation of woven all-silk composites (ASCs),[92] and silk fibroin,[93] for nanoparticle synthesis, silk fiber dissolution, and wool fiber treatment.[94] Microwave heating, due to its rapid energy transfer, was expected to enhance protein breakdown;[95,96] however, this was not the case. One possible explanation is that high-intensity microwaves caused localized overheating, leading to partial degradation of both proteins and the biopolymer, generating byproducts that interfered with the extraction process and reduced final purity. Another

possibility is that the short exposure time—chosen to preserve chitin integrity—was insufficient for the complete hydrolysis of peptide bonds.

Pulping with [C$_4$mim][HSO$_4$] was inherently less effective in protein solubilization than acetate-based ILs likely due to the presence of acidic hydrogen sulfate anions ([HSO$_4$]$^-$, pH ~2–3 in aqueous solutions), incapable of disrupting protein structures. Additionally, proteins tend to precipitate in acidic conditions, as low pH promotes aggregation rather than solubilization,[97] and could co-precipitate with chitin.

**TGA and Derivative Thermogravimetric Analysis (DTG)** were used to provide detailed insights into the purity of the isolated materials. DTG, which plots the rate of mass change with respect to temperature, allows for a more detailed analysis of the thermal events observed in the TGA data. By comparing the maximum degradation temperatures (DTG$_{max}$) obtained from the DTG curve with the mass loss data from TGA, we can further confirm the purity of the material. All chitin types displayed a two-step decomposition process (Fig. S16, ESI†). The first step, occurring at 50–100 °C, is attributed to water evaporation, while the second step, between 250–400 °C, corresponds to carbohydrate degradation. The thermograms and DTG plots (Fig. S16 and S17, ESI†), the maximum degradation peaks (DTG$_{max}$, Table 2), and the water and ash content were determined. The DTG$_{max}$ values for the samples show significant differences in thermal stability based on their thermal degradation behavior. Wh/Chitin$_{NaOH-24}$ exhibits the highest DTG$_{max}$ of 348.6 °C, indicating it is the most thermally stable sample, likely due to its highest purity. Wh/Chitin$_{[C_2mim][OAc] \; Thermal}$ follows closely with a DTG$_{max}$ of 343.9 °C, showing similar thermal stability, implying a similar purity. Wh/Chitin$_{NaOH-2}$ and Wh/Chitin$_{[C_2mim][OAc] \; Microwave}$ exhibit a DTG$_{max}$ of 324.1 and 322.6 °C, respectively, indicating similar thermal degradation characteristics between these two samples and suggesting a significantly reduced thermal stability compared to Wh/Chitin$_{NaOH-24}$ and Wh/Chitin$_{[C_2mim][OAc] \; Thermal}$. The sample Wh/Chitin$_{[C_4mim][HSO_4]}$ shows a DTG$_{max}$ of 309.2 °C, pointing to lower thermal stability, potentially due to higher impurity content. Finally, Wh/Chitin$_{DES}$ has the lowest DTG$_{max}$ of 300.9 °C, suggesting the least thermal stability and indicating the highest amount of impurities compared to the other samples. Overall the decomposition temperature trend was the same as the purity trend seen by $^{13}$C multiCP-MAS NMR: Wh/Chitin$_{NaOH-24}$ ≈ Wh/Chitin$_{[C_2mim][OAc] \; Thermal}$ > Wh/Chitin$_{NaOH-2}$ ≈ Wh/Chitin$_{[C_2mim][OAc] \; Microwave}$ > Wh/Chitin$_{[C_4mim][HSO_4]}$ > Wh/Chitin$_{DES}$.

In comparison with literature values, Hassainia *et al.* reported a DTG$_{max}$ of 309 °C for an isolate from white mushrooms,[80] and Wu *et al.* obtained a similar maximum decomposition temperature of 310 °C for the same mushroom.[60] Boureghda *et al.* found the maximum thermal decomposition for chitin–glucan complex from white mushrooms to be 300 °C.[72] The values obtained in our study align with these reports, suggesting that the purity of Wh/Chitin$_{[C_4mim][HSO_4]}$ is comparable to that reported by Hassainia *et al.*, who described relatively impure chitin. In contrast, the DTG$_{max}$ value for

Wh/Chitin$_{DES}$ suggests the presence of chitin–glucan complex. The variations observed in DTG$_{max}$ values can be attributed to differences in extraction methods and the purity of the isolates.

The extraction results revealed notable differences in yield, purity, and chitin recovery across the various methods employed. The DES method achieved the highest crude yield (30.6 ± 1.4%), followed by NaOH-2 (27.1 ± 8.0%) and [C$_4$mim][HSO$_4$] (23.8 ± 0.4%). Conversely, the NaOH-24 and thermal [C$_2$mim][OAc] methods produced lower crude yields, reflecting their emphasis on purity over quantity. In terms of purity, the NaOH-24 and thermal [C$_2$mim][OAc] methods excelled, each yielding chitin with 77.0% purity, suitable for applications requiring high-quality material. On the other hand, the DES method resulted in the lowest purity (29.8%). Across all methods, the amount of chitin in crude material consistently ranged from 7.7% to 9.5%, accounting for variability within the error margins. This suggests relatively stable chitin content, regardless of the extraction method, but with substantial differences in purity.

### Additional characterization

**Powder X-ray diffraction (PXRD)** was employed to determine the crystallinity of each product, as this is a key parameter for chitin characterization. As is well known, crystallinity plays a crucial role in determining the structural, mechanical, thermal, and functional properties of materials, making its evaluation essential for optimizing material preparation. Higher crystallinity typically results in greater rigidity, tensile strength, and resistance to deformation, as the ordered molecular structure enhances intermolecular interactions, such as hydrogen bonding in biopolymers like chitin. Conversely, lower crystallinity materials tend to be more flexible and ductile, which can be advantageous in applications requiring pliability. Given its significant impact on material properties, we proceeded with the evaluation of crystallinity of chitin extracted by different methods.

The diffractograms of all chitinous fractions were compared to the commercial chitin and glucan diffractograms and the diffractograms from the starting biomass (Fig. S18, ESI†). For crude biomass, the peaks were located at 9.7, 19.5, 20.4, 21.1, 22.0, 25.1, 28.1, 30.7, 34.8, 36.0, 40.4, and 44.7° 2θ. Literature suggests six peaks prominent for α-chitin, at 2θ 9.3, 12.7, 19.3, 20.5, 23.2, and 26.3°,[98,99,100] that correspond to the crystalline planes (020), (021), (110), (120), (130), and (013), suggesting a typical α-chitin crystalline structure. Specifically for mushrooms, studies reported 9.6, 19.6, 21.1 and 23.7° for α-chitin, 9.1 and 20.3° for β-chitin and 9.6 and 19.8° for γ-chitin,[101] while the rest of the peaks are associated with minerals. After all treatments, a significant amount of minerals was visibly removed from the isolated chitinous fraction when compared to the original biomass. Peaks at ~9, 19.5°, and 26.6° 2θ, corresponding to the (020), (110), and (013) chitin crystalline lattice planes, respectively, were found across all samples.

The crystallinity index (%CrI) was determined using the peak deconvolution method, which calculates the ratio between the area of crystalline peaks and the total area of the PXRD spectrum for improved accuracy.[102,103] The highest %CrI was observed for Wh/Chitin$_{NaOH}$ with slightly more crystalline material when longer treatment time was employed, with values of 80.3 and 84.8% for 2 and 24 h treatment, respectively. Dissolution in [C$_2$mim][OAc] is known to provide highly amorphous materials because the IL disrupts the regular, ordered crystalline structure of chitin. This disruption breaks down intermolecular hydrogen bonds, leading to a loss of crystallinity. As expected, Wh/Chitin$_{[C_2mim][OAc]}$ exhibited a reduced crystallinity of 66.1%, for microwave-assisted dissolution and 64.5% for thermal dissolution. DES resulted in highly amorphous materials, with %CrI 61%. Finally, Wh/Chitin$_{[C_4mim][HSO_4]}$ was 63.3% crystalline.

The size of crystallites affects properties like mechanical strength, hardness, and thermal stability. For instance, materials with smaller crystallites often exhibit higher hardness. The crystallite size for isolated Wh/Chitin$_{NaOH-24}$ and Wh/Chitin$_{NaOH-2}$, were calculated for two prominent peaks at the (020) and (110) planes by Scherrer's equation[75] and are provided in Table 2. The crystallite size at the plane of (020) ranges from 3.9 nm to 4.7 nm for samples extracted by NaOH. For samples isolated by extraction with [C$_2$mim][OAc], the crystallite size was found to be 3.8 nm, at the plane (020) and 3.5 nm, at the plane (110). The crystallite size of Wh/Chitin$_{[C_4mim][HSO_4]}$ was measured as 2.7 and 4.9 nm at the (110) and (020) planes, respectively. For Wh/Chitin$_{DES}$, the crystallite size was found to be 3.8 nm at the (020) and 4.2 nm at the (110) plane, respectively.

**Relative molecular weight.** Viscosity is one of the major quality criteria for industrial applications of chitin. To produce materials from chitin polymer, achieving a certain viscosity is crucial, as it directly influences the processability and quality of the final product. For instance, in extrusion applications, chitin solutions are extruded through a nozzle of the syringe or needle tip into a coagulation bath, where the polymer solidifies into fibers.[104] The viscosity of the polymer solution must be carefully controlled for successful wet jet extrusion, as it significantly impacts the fiber formation, structure, and quality. If the viscosity is too high, the polymer may solidify too slowly upon entering the coagulation bath, resulting in fiber deformations. On the other hand, if the viscosity is too low, it can lead to an interrupted flow, producing short and discontinuous fibers. In addition to influencing fiber formation, viscosity plays a critical role in determining the mechanical properties of polymer-based materials, such as tensile strength, by affecting the alignment of polymer chains, which in turn impacts the overall structural integrity of the material.

To compare practical implications for processing, the viscosities of solutions of 2.5 wt% chitin obtained from shrimp shells using [C$_2$mim][OAc][66] and the two purest fungal chitins, *i.e.*, Wh/Chitin$_{NaOH-24}$ and Wh/Chitin$_{[C_2mim][OAc] Thermal}$ in [C$_2$mim][OAc], were determined at different temperatures to compare their relative Mw. The data (Fig. 4) indicated comparable viscosities of the solutions Wh/Chitin$_{NaOH-24}$, Wh/Chitin$_{[C_2mim][OAc] Thermal}$, and crustacean chitin obtained
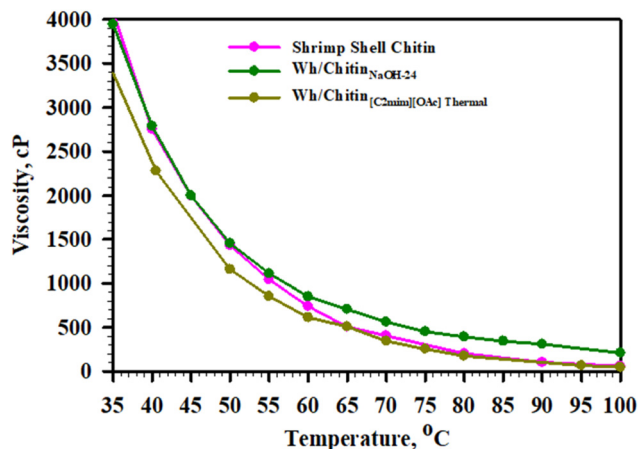
**Fig. 4** Viscosity measurements for 2.5 wt% [C₂mim][OAc] solutions of shrimp shell chitin extracted with [C₂mim][OAc] (pink), mushroom chitin pulped with NaOH for 24 h (dark green), and mushroom chitin extracted with [C₂mim][OAc]–thermal (olive).

using the same protocol. The results may indicate that the Mw of the isolated fungal chitin is similar to that recovered from crustaceans.

### Chitinous materials – preparation and characterization of chitinous fibers

The isolated fungal chitins of the highest purity, Wh/Chitin$_{NaOH-24}$ and Wh/Chitin$_{[C_2mim][OAc]\ Thermal}$, were dissolved in [C₂mim][OAc] at 2.5 wt% concentration. The solutions were then transferred into a 12 mL plastic syringe (14 mm diameter) to extrude fibers into a coagulation bath containing 1–1.5 L deionized water. The syringe, connected to a syringe pump, extruded fibers at a 1.6 mL min⁻¹ rate with the syringe tip about 2 mm above the water surface. The fibers were collected on an empty centrifuge tube, washed 10 times with DI water, and dried for further analysis. It's important to note the absence of rotating rollers used in fiber spinning to control the tension and speed of the fibers as they are drawn out (godets). Godets are typically used to stretch and draw fibers after they are extruded aligning the polymer chains along the fiber axis. Without godets, weaker fibers are produced.

The SEM images of the prepared fibers indicated a smooth fiber surface (Fig. S19 and S20, ESI†), usually correlated to pure biopolymers used in the preparation of the materials.[105] The stress–strain relationship for Wh/Chitin$_{NaOH-24}$ and Wh/Chitin$_{[C_2mim][OAc]\ Thermal}$ white mushroom chitin fibers was then determined and compared with fibers prepared from shrimp shell chitin drawn under identical conditions using the same setup (Fig. S21, ESI†).

According to our previous studies, the strength values for the chitin fibers could roughly be separated into three groups: fibers from shrimp biomass (strength 80–90 MPa), crab and lobster biomass (50–70 MPa), and fly larvae biomass (14 MPa).[106] However, the reported results were obtained using

**Table 3** Tensile strength data of the fibers produced using different sources of chitin

| Chitin source | Strength (MPa) | Elongation (%) |
|---|---|---|
| SS Chitin[a] | 28.1 ± 2.2[A] | 5.6 ± 1.5[A] |
| Wh/Chitin$_{NaOH-24}$ | 25.2 ± 4.9[A,B] | 5.5 ± 0.5[A] |
| Wh/Chitin$_{[C_2mim][OAc]\ Thermal}$ | 23.1 ± 1.4[B] | 3.0 ± 0.8[B] |

[a] SS Chitin is the polymer extracted from shrimp shells using [C₂mim][OAc]. [A,B]Groups with the same letter are not detectably different (are in the same set) and groups that are detectably different get different letters (different sets).

different fiber drawing conditions and, importantly, setup. To ensure that any observed differences were not artifacts of the experimental setup, we have extracted chitin from shrimp shell biomass using [C₂mim][OAc], and prepared fibers to be used as a control. This allowed us to account for potential influences from the experimental setup itself and compare the strengths of fibers prepared from shrimp shell chitin and mushroom chitin, isolated using the same IL, and mushroom chitin isolated using NaOH.

It was found that the tensile strength of fibers made from shrimp shell chitin (28.1 ± 2.2 MPa) and Wh/Chitin$_{NaOH-24}$ (25.2 ± 4.9 MPa) is not statistically different (Table 3). Similarly, the strength values for Wh/Chitin$_{NaOH-24}$ and Wh/Chitin$_{[C_2mim][OAc]\ Thermal}$ fibers (25.2 ± 4.9 MPa and 23.1 ± 1.4 MPa, respectively) are statistically comparable. However, fibers prepared from shrimp shell chitin exhibit a statistically significant, albeit slight, strength advantage over Wh/Chitin$_{[C_2mim][OAc]\ Thermal}$ fungal chitin fibers. In respect to elongation, the values of fibers prepared from shrimp shell chitin (5.6 ± 1.5%) and Wh/Chitin$_{NaOH-24}$ (5.5 ± 0.5%) are not statistically different, as indicated by the same letter in Table 3. However, the elongation value for Wh/Chitin$_{[C_2mim][OAc]\ Thermal}$ fibers (3.0 ± 0.8%) is significantly lower than both shrimp shell chitin and Wh/Chitin$_{NaOH-24}$ fibers, as denoted by a different letter in Table 3.

## Conclusions

This study presents a comprehensive analysis of various extraction methods for isolating chitin from white mushrooms, providing a deeper understanding of the trade-offs between yield, purity, and crystallinity. Fungal chitin represents a forward-thinking, sustainable, and ethical alternative to animal-derived chitin. Its adoption in various C-based materials industries can appeal to environmentally conscious consumers and advocates of animal welfare. Fungal chitin is abundant, scalable, and grows on waste substrates, making it an environmentally friendly option that supports the circular economy.

The comparison of various chitin extraction methods and the resulting material properties highlights key findings and practical implications for applications requiring purified 'vegan' non-allergenic chitin. By evaluating both conventional and environmentally friendly approaches, such as IL-based

extractions, this work highlights the potential of fungal biomass as a sustainable and hypoallergenic source of chitin. The findings demonstrate the unsuitability of certain methods, like DES, for the purification of fungal chitin, while others, like thermal IL treatments, excel in purity and structural integrity, offering insights into tailoring extraction processes for specific applications.

The use of NaOH and $[C_2mim][OAc]$ (under oil heating) treatments produced the highest-purity chitin samples, with both methods showing similar degrees of acetylation, crystallinity, and thermal stability. Notably, the solutions of these samples in $[C_2mim][OAc]$ also exhibited comparable viscosities to a $[C_2mim][OAc]$ solution of shrimp shell-derived chitin at the same, 2.5 wt% concentration, which is significant for processing and fabrication in industrial applications. However, there is a notable distinction in the environmental and safety implications of the extraction methods.

IL-based methods, particularly those utilizing $[C_2mim][OAc]$, provide a more environmentally-benign alternative to conventional NaOH treatments. A key advantage in green chemistry is the replacement of hazardous chemicals traditionally used for fungal chitin isolation (*e.g.*, HCl and NaOH) with an ionic liquid solvent classified under the lowest toxicity category (GHS Category 5[107]). In addition, $[C_2mim][OAc]$ is regarded as a more environmentally-benign alternative.[108] It is less toxic, non-corrosive, and its recovery and reuse are feasible, making it a more sustainable option. Besides, $[C_2mim][OAc]$ is considered innocuous under normal handling conditions, reducing health and safety risks compared to NaOH-based methods.[109]

The use of NaOH, particularly in high concentrations, can be hazardous. Sodium hydroxide is a strong alkali that, when improperly handled, poses risks such as severe burns and environmental harm, especially in large-scale industrial applications where waste disposal and neutralization become significant concerns. However, a comprehensive quantitative sustainability assessment remains necessary, incorporating metrics such as *E*-factor, atom economy, life cycle analysis (LCA), and energy consumption to fully evaluate its environmental impact.

Although IL-based extraction requires similar energy input to NaOH-based methods, it achieves comparable chitin purity while offering significant environmental benefits, including reduced corrosive waste generation, enhanced solvent recyclability, and improved process safety. Thus, while not inherently more energy-efficient, the IL-based approach aligns with sustainability principles by minimizing hazardous byproducts.

It is important to emphasize the need for ionic liquid (IL) recyclability, which is a critical factor in the sustainability and economic feasibility of any IL-based process.[37] Efficient IL recovery and reuse can significantly reduce costs and minimize environmental impact. Various strategies, such as solvent extraction, distillation, membrane separation, and electrochemical methods, have been explored to recover ILs while maintaining their functional properties.[37] In chitin extraction and related applications, optimizing IL recycling techniques can enhance process sustainability and mitigate waste generation. However, challenges remain in terms of purity retention, degradation over multiple cycles, and energy consumption during recovery. Future research on fungal chitin should focus on refining IL recycling strategies to ensure high recovery rates while preserving the efficiency of ILs in biopolymer processing.

Interestingly, the incorporation of more aggressive methods, such as microwave heating into the extraction process, while potentially offering faster extraction times and energy savings, does not necessarily provide superior purity, as evidenced by both NMR and thermogravimetric analyses. The same was the case when using the acidic IL $[C_4mim][HSO_4]$. Among the treatments, the DES-based method yielded the lowest purity, due to incomplete removal of glucan impurities, making it unsuitable for chitin isolation.

In terms of physical properties, chitin extracted from mushrooms exhibited good mechanical performance when spun into fibers, although the strength of fungal chitin fibers was lower than that of fibers from crustacean sources. Nonetheless, fungal chitin fibers, particularly those isolated by NaOH-24 and thermal $[C_2mim][OAc]$ treatments, showed promising tensile strength and elongation characteristics, indicating their potential for various applications in biocomposite materials, biomedical devices, and biodegradable fibers.

Although fungal chitin extraction with $[C_2mim][OAc]$ shows promise, the technology remains less mature than the same extraction processes for chitin from crustacean shells, and significantly less mature than 'traditional' chitin pulping which benefit from well-established supply chains and infrastructure optimized for high-yield and cost-effective production. These processes have reached a level of technological maturity that allows for large-scale, economically viable (ignoring future, more restrictive environmental regulations) production, primarily due to the widespread availability of crustacean waste as a raw material. Conversely, fungal chitin production is still largely experimental, with most processes operating at a lab scale. Challenges related to production costs, cultivation conditions, and technology transfer hinder its large-scale commercialization, despite its potential environmental benefits.

The practical significance of this work is underscored by its sustainability benefits, material performance in biopolymer applications, and relevance as an alternative to crustacean-derived chitin. The use of ILs, particularly $[C_2mim][OAc]$, reduces hazardous waste production and enables solvent recyclability, making IL-based extraction a viable option for industries prioritizing environmentally-responsible biopolymer production. The extracted fungal chitin demonstrated structural properties suitable for fiber formation, indicating potential applications in biodegradable packaging, biomedical materials, and sustainable textiles. Furthermore, this study confirms that fungal chitin achieves comparable purity and structural integrity to crustacean-derived chitin, making it a viable alternative for industries seeking vegan, non-allergenic, and biomedical applications.

To enhance the industrial applicability of this method, future research should focus on optimizing reaction conditions, refining purification protocols to selectively remove

residual proteins while preserving chitin integrity, and conducting IL recovery studies, along with assessing the scalability of this technology for large-scale applications, including industrial infrastructure requirements. A comprehensive techno-economic analysis (TEA) is also essential, encompassing cost estimation of raw materials and reagents, energy consumption and process efficiency assessments, and waste management and environmental impact evaluations. While these aspects extend beyond the scope of this study and require detailed economic modeling, process optimization, and lifecycle analysis, our findings establish a foundation for future techno-economic studies that could evaluate the economic feasibility and scalability of IL-based chitin extraction compared to conventional methods.

Although currently at a lab-scale stage, fungal chitin extraction shows strong potential for industrial adoption, with promising opportunities for process optimization, scalability assessments, and cost evaluations. Furthermore, the utilization of waste-derived fungal biomass further strengthens its case as a sustainable alternative in biopolymer production, offering both environmental and economic benefits for future large-scale applications.

By addressing key challenges in fungal chitin extraction, this work opens new avenues for research in biopolymer recovery from alternative biomass sources, such as fungi. Future studies could explore optimizing environmentally conscious methods to improve scalability and reduce costs. Additionally, expanding research into diverse biomass species and integrating a biomass-agnostic technology for manufacture of C-based materials for various industries can further advance the sustainability of chitin isolation and reduce exclusive reliance on crustacean-derived sources.

Overall, this study illustrates that while the choice of extraction method significantly influences the purity, thermal stability, and mechanical properties of fungal chitin, it is possible to achieve high-quality chitin comparable to traditional sources like shrimp shells. Further research focusing on optimizing extraction processes and enhancing material properties could expand the potential for sustainable chitin production from fungal biomass, while also minimizing environmental and health risks associated with the extraction process.

## Author contributions

Conceptualization, J. L. S. and P. B.; methodology, J. L. S.; data collection and analysis, A. Z., B. W., and J. L. S.; writing – original draft preparation, A. Z., J. L. S. and P. B.; writing – review and editing, J. L. S., P. B., and R. D. R.; supervision, J. L. S.; funding acquisition, J. L. S. All authors have read and agreed to the published version of the manuscript.

## Data availability

The original contributions presented in the study are included in the article/ESI.† Further inquiries can be directed to the corresponding authors.

## Conflicts of interest

The authors declare the following competing financial interests: Robin D. Rogers is a named inventor on related patents and applications and has partial ownership of 525 Solutions, Inc. and Wyonics LLC. J. L. Shamshina is an inventor of related patents and applications, a former employee of 525 Solutions, Inc., and has partial ownership of Chitalyst, LLC.

## Acknowledgements

## References

1  V. Zargar, M. Asghari and A. Dashti, *ChemBioEng Rev.*, 2015, **2**, 204–226.
2  R. Jayakumar, K. P. Chennazhi, S. Srinivasan, S. V. Nair, T. Furuike and H. Tamura, *Int. J. Mol. Sci.*, 2011, **12**, 1876–1887.
3  B. K. Park and M. M. Kim, *Int. J. Mol. Sci.*, 2010, **11**, 5152–5164.
4  J. L. Shamshina, A. Kelly, T. Oldham and R. D. Rogers, *Environ. Chem. Lett.*, 2020, **18**, 53–60.
5  Z. Yu, Y. Ji, V. Bourg, B. Mustafa and J. C. Meredith, *Emergent. Mater.*, 2020, **3**, 919–936.
6  J. Liao, Y. Zhou, B. Hou, J. Zhang and H. Huang, *Carbohydr. Polym.*, 2023, **305**, 120553.
7  C. Casadidio, D. V. Peregrina, M. R. Gigliobianco, S. Deng, R. Censi and P. Di Martino, *Mar. Drugs*, 2019, **17**, 369.
8  H. Amiri, M. Aghbashlo, M. Sharma, J. Gaffey, L. Manning, S. M. M. Basri, J. F. Kennedy, V. K. Gupta and M. Tabatabaei, *Nat. Food*, 2022, **3**, 822–828.
9  X. Dong, L. Shi, S. Ma, X. Chen, S. Cao, W. Li, Z. Zhao, C. Chen and H. Deng, *Nano Lett.*, 2024, **24**, 12014–12026.
10  Fishery Statistical Collections, Food and Agriculture Organization of the United Nations, **https://www.fao.org/fishery/statistics/global-production**, (accessed 30 November 2024).
11  Z. Zhang, Z. Ma, L. Song and M. A. Farag, *J. Adv. Res.*, 2024, **57**, 59–76.
12  C. King, R. S. Stein, J. L. Shamshina and R. D. Rogers, *ACS Sustainable Chem. Eng.*, 2017, **5**, 8011–8016.
13  A. Venkatachalam, M. B. Govinda Rajulu, N. Thirunavukkarasu and T. S. Suryanarayanan, *Mycosphere*, 2015, **6**, 345–355.
14  F. J. Alvarez, *Molecules*, 2014, **19**, 4433–4451.
15  U. Bose, J. A. Broadbent, A. Juhász, S. Karnaneedi, E. B. Johnston, S. Stockwell, K. Byrne, V. Limviphuvadh, S. Maurer-Stroh, A. L. Lopata and M. L. Colgrave, *J. Proteomics*, 2022, **269**, 104724.

16 S. H. Sicherer, A. Muñoz-Furlong and H. A. Sampson, *J. Allergy Clin. Immunol.*, 2004, **114**, 159–165.

17 V. Ghormade, E. K. Pathan and M. V. Deshpande, *Int. J. Biol. Macromol.*, 2017, **104**, 1415–1421.

18 Sangeeta, D. Sharma, S. Ramniwas, R. Mugabi, J. Uddin and G. A. Nayik, *Food Chem.: X*, 2024, **23**, 101774.

19 T. Huq, A. Khan, D. Brown, N. Dhayagude, Z. He and Y. Ni, *J. Bioresour. Bioprod.*, 2022, **7**, 85–98.

20 R. Radulovich and J. P. Fuentes-Quesada, *Aquaculture*, 2019, **512**, 734354.

21 E. I. Díaz-Rojas, W. M. Argüelles-Monal, I. Higuera-Ciapara, J. Hernández, J. Lizardi-Mendoza and F. M. Goycoolea, *Macromol. Biosci.*, 2006, **6**(5), 340–347.

22 X. Hu, Z. Tian, X. Li, S. Wang, H. Pei, H. Sun and Z. Zhang, *ACS Omega*, 2020, **5**(30), 19227–19235.

23 R. Amelia, N. M. Saptarini, E. Halimah, Y. Andriani, A. Nurhasanah, J. Levita and S. A. Sumiwi, *J. Appl. Pharm. Sci.*, 2020, **10**(12), 140–149.

24 I. Ofenbeher-Miletić, D. Stanimirović and S. Stanimirović, *Plant Foods Hum. Nutr.*, 1984, **34**, 197–201, DOI: 10.1007/BF01091469.

25 M. A. Rahman, S. Bhuiyan, S. Shakil and S. Hossain, *J. Biomed. Res.*, 2023, **4**(1), 25–28.

26 X. Kang, A. Kirui, A. Muszyński, M. C. D. Widanage, A. Chen, P. Azadi, P. Wang, F. Mentink-Vigier and T. Wang, *Nat. Commun.*, 2018, **9**, 1–12.

27 I. Chakraborty, S. Mondal, D. Rout and S. S. Islam, *Carbohydr. Res.*, 2006, **341**, 2990–2993.

28 M. A. Wickramasinghe, H. Nadeeshani, S. M. Sewwandi, I. Rathnayake, T. C. Kananke and R. Liyanage, *Food Prod., Process. Nutr.*, 2023, **5**, 43, DOI: 10.1186/s43014-023-00158-9.

29 S. E. Mallikarjuna, A. Ranjini, D. J. Haware, M. R. Vijayalakshmi, M. N. Shashirekha and S. Rajarathnam, *J. Chem.*, 2013, **2013**, 805284, DOI: 10.1155/2013/805284.

30 B. T. Iber, N. A. Kasan, D. Torsabo and J. W. Omuwa, *J. Renewable Mater.*, 2022, **10**, 1097–1123, DOI: 10.32604/JRM.2022.018142.

31 H. El Knidri, R. Belaabed, A. Addaou, A. Laajeb and A. Lahsini, *Int. J. Biol. Macromol.*, 2018, **120**, 1181–1189.

32 N. A. Z. Abidin, F. Kormin, N. A. Z. Abidin, N. A. F. M. Anuar and M. F. A. Bakar, *Int. J. Mol. Sci.*, 2020, **21**, 4978.

33 X. Yang, J. Liu, Y. Pei, X. Zheng and K. Tang, *Energy Environ. Mater.*, 2020, **3**, 492–515, DOI: 10.1002/eem2.12079.

34 K. Mohan, A. R. Ganesan, P. N. Ezhilarasi, K. K. Kondamareddy, D. K. Rajan, P. Sathishkumar, J. Rajarajeswaran and L. Conterno, *Carbohydr. Polym.*, 2022, **287**, 119349, DOI: 10.1016/j.carbpol.2022.119349.

35 K. Morgan, C. Conway, S. Faherty and C. Quigley, *Molecules*, 2021, **26**, 7603, DOI: 10.3390/molecules26247603.

36 I. Younes, O. Ghorbel-Bellaaj, R. Nasri, M. Chaabouni, M. Rinaudo and M. Nasri, *Process Biochem.*, 2012, **47**, 2032–2039, DOI: 10.1016/j.procbio.2012.07.017.

37 J. L. Shamshina, *Green Chem.*, 2019, **21**, 3974–3993, DOI: 10.1039/C9GC01830A.

38 G. P. Rachiero, P. Berton and J. Shamshina, *Molecules*, 2022, **27**, 6606, DOI: 10.3390/molecules27196606.

39 M. Borić, H. Puliyalil, U. Novak and B. Likozar, *Green Chem.*, 2018, **20**, 1199–1204.

40 R. Devi and R. Dhamodharan, *ACS Sustainable Chem. Eng.*, 2018, **6**, 846–853.

41 H. Yang, G. Gözaydın, R. R. Nasaruddin, J. R. G. Har, X. Chen, X. Wang and N. Yan, *ACS Sustainable Chem. Eng.*, 2019, **7**(5), 5532–5542.

42 O. Ghorbel-Bellaaj, I. Younes, H. Maâlej, S. Hajji and M. Nasri, *Int. J. Biol. Macromol.*, 2012, **51**, 1196–1201.

43 X. Chen, S. Song, H. Li, G. Gözaydın and N. Yan, *Acc. Chem. Res.*, 2021, **54**, 1711–1722, DOI: 10.1021/acs.accounts.0c00842.

44 J. L. Shamshina and P. Berton, *Front. Bioeng. Biotechnol.*, 2020, **8**, DOI: 10.3389/fbioe.2020.00011.

45 S. Nikolov, H. Fabritius, M. Petrov, M. Friák, L. Lymperakis, C. Sachs, D. Raabe and J. Neugebauer, *J. Mech. Behav. Biomed. Mater.*, 2011, **4**, 129–145, DOI: 10.1016/j.jmbbm.2010.09.015.

46 A. Chakraborty, L. D. Fernando, W. Fang, M. C. D. Widanage, P. Wei, C. Jin, T. Fontaine, J. P. Latgé and T. Wang, *Nat. Commun.*, 2021, **12**, 6346, DOI: 10.1038/s41467-021-26749-z.

47 S. P. O. Álvarez, D. A. R. Cadavid, D. M. E. Sierra, C. P. O. Orozco, D. F. R. Vahos, P. Z. Ocampo and L. Atehortúa, *BioMed. Res. Int.*, 2014, **2014**, 169071.

48 T. N. Ivshina, S. D. Artamonova, V. P. Ivshin and F. F. Sharnina, *Appl. Biochem. Microbiol.*, 2009, **45**, 313–318.

49 K. J. Kasongo, D. J. Tubadi, L. D. Bampole, T. A. Kaniki, N. J. M. Kanda and M. E. Lukumu, *SN Appl. Sci.*, 2020, **2**, 406.

50 R. A. A. Muzzarelli, P. Ilari, R. Tarsi, B. Dubini and W. Xia, *Carbohydr. Polym.*, 1994, **25**, 45–50.

51 A. Fadhil and E. F. Mous, *IOP Conf. Ser. Earth Environ. Sci.*, 2021, **761**, 012127.

52 N. M. Ospina, S. P. O. Alvarez, D. M. E. Sierra, D. F. Vahos, P. A. Z. Ocampo and C. P. O. Orozco, *J. Mater. Sci. Mater. Med.*, 2015, **26**, 135.

53 S. Erdogan, M. Kaya and I. Akata, *AIP Conf. Proc.*, 2017, **1809**, 020012.

54 W. Wang, Y. Du, Y. Qiu, X. Wang, Y. Hu, J. Yang, J. Cai and J. F. Kennedy, *Carbohydr. Polym.*, 2008, **74**, 127–132.

55 S. Ifuku, R. Nomura, M. Morimoto and H. Saimoto, *Materials*, 2011, **4**, 1417–1425.

56 C. Burballa, M. Crespo, D. Redondo-Pachón, M. J. Pérez-Sáez, C. Arias-Cabrales, M. Mir, A. Francés, L. Fumadó, L. Cecchini and J. Pascual, *Nefrologia*, 2018, **38**, 528–534.

57 M. Kannan, M. Nesakumari and K. Rajarathinam, *Adv. Biol. Res.*, 2010, **4**, 10–13.

58  T. Wu, S. Zivanovic, F. A. Draughon and C. E. Sams, *J. Agric. Food Chem.*, 2004, **52**, 7905–7910.

59  T. Wu, S. Zivanovic, F. A. Draughon, W. S. Conway and C. E. Sams, *J. Agric. Food Chem.*, 2005, **53**, 3888–3894.

60  J. Wu, Y. Niu, Y. Jiao and Q. Chen, *Int. J. Biol. Macromol.*, 2019, **123**, 291–299.

61  J. Liao and H. Huang, *Int. J. Biol. Macromol.*, 2020, **156**, 1279–1286.

62  F. Di Mario, P. Rapanà, U. Tomati and E. Galli, *Int. J. Biol. Macromol.*, 2008, **43**, 8–12.

63  J. L. Shamshina, P. S. Barber, G. Gurau, C. S. Griggs and R. D. Rogers, *ACS Sustainable Chem. Eng.*, 2016, **4**, 6072–6081.

64  R. Sulthan, A. Reghunadhan and S. Sambhudevan, *J. Mol. Liq.*, 2023, **380**, 121794.

65  L. D. Tolesa, B. S. Gupta and M. J. Lee, *Int. J. Biol. Macromol.*, 2019, **130**, 818–826.

66  Y. Qin, X. Lu, N. Sun and R. D. Rogers, *Green Chem.*, 2010, **12**, 968–997.

67  K. Morgan, C. Conway, S. Faherty and C. Quigley, *Molecules*, 2021, **26**, 7603.

68  P. Zhu, Z. Gu, S. Hong and H. Lian, *Carbohydr. Polym.*, 2017, **177**, 217–223.

69  G. P. Rachiero, P. Berton and J. Shamshina, *Molecules*, 2022, **27**, 1–14.

70  A. Zannat and J. L. Shamshina, *Carbohydr. Polym.*, 2025, **348**, 122882.

71  J. L. Shamshina and N. Abidi, *ACS Sustainable Chem. Eng.*, 2022, **10**, 11846–11855.

72  Y. Boureghda, H. Satha and F. Bendebane, *Waste Biomass Valorization*, 2021, **12**, 6139–6153.

73  A. S. Shkuratov, R. P. Shibu, O. Therasme, P. Berton and J. L. Shamshina, *Sustainable Chem.*, 2024, **5**, 130–148.

74  P. S. Saravana, T. C. Ho, S.-J. Chae, Y.-J. Cho, J.-S. Park, H.-J. Lee and B.-S. Chun, *Carbohydr. Polym.*, 2018, **195**, 622–630.

75  P. Scherrer, *Nachr. Ges. Wiss. Gottingen*, 1918, **2**, 98–100.

76  Y. Fan, H. Fukuzumi, T. Saito and A. Isogai, *Int. J. Biol. Macromol.*, 2012, **50**, 69–76.

77  ASTM D3822-07 Standard Test Method for Tensile Properties of Single Textile Fibers. Available at: https://compass.astm.org/document/?contentCode=ASTM%7CD3822-07%7Cen-US&proxycl=https%3A%2F%2Fsecure.astm.org&fromLogin=true, accessed 11 December 2024.

78  M. Broz, C. Oostenbrink and U. Bren, *J. Chem. Inf. Model.*, 2024, **64**, 2077–2083.

79  R. P. Swatloski, S. K. Spear, J. D. Holbrey and R. D. Rogers, *J. Am. Chem. Soc.*, 2002, **124**, 4974–4975.

80  A. Hassainia, H. Satha and S. Boufi, *Int. J. Biol. Macromol.*, 2018, **117**, 1334–1342.

81  J. Liu, X. Zhang, J. Zhang, M. Yan, D. Li, S. Zhou, J. Feng and Y. Liu, *Polymers*, 2022, **14**, 549.

82  J. Kumirska, M. Czerwicka, Z. Kaczyński, A. Bychowska, K. Brzozowski, J. Thöming and P. Stepnowski, *Mar. Drugs*, 2010, **8**, 1567–1636.

83  E. Brunner, H. Ehrlich, P. Schupp, R. Hedrich, S. Hunoldt, M. Kammer, S. Machill, S. Paasch, V. V. Bazhenov, D. V. Kurek, T. Arnold, S. Brockmann, M. Ruhnow and R. Born, *J. Struct. Biol.*, 2009, **168**, 539–547.

84  B. Focher, A. Naggi, G. Torri, A. Cosani and M. Terbojevich, *Carbohydr. Polym.*, 1992, **17**, 97–102.

85  F. G. Pearson, R. H. Marchessault and C. Y. Liang, *J. Polym. Sci.*, 1960, **43**, 101–116.

86  A. Oberemko, A. M. Salaberria, R. Saule, G. Saulis, M. Kaya, J. Labidi and V. Baublys, *Carbohydr. Polym.*, 2019, **221**, 1–9.

87  M. M. Black and H. M. Schwartz, *Analyst*, 1950, **889**, 185–189.

88  Y. Yamanoi and M. Hattori, *Bull. Chem. Soc. Jpn.*, 2024, **97**, 1–7.

89  G. Galed, B. Miralles, I. Paños, A. Santiago and Á. Heras, *Carbohydr. Polym.*, 2005, **62**, 316–320.

90  M. R. Kasaai, *Carbohydr. Polym.*, 2010, **79**, 801–810.

91  Y. Xu, M. Bajaj, R. Schneider, S. L. Grage, A. S. Ulrich, J. Winter and C. Gallert, *Microb. Cell Fact.*, 2013, **12**, 90.

92  X. Zhang, M. E. Ries and P. J. Hine, *Compos. Sci. Technol.*, 2023, **239**, 110046.

93  X. Zhang, M. E. Ries and P. J. Hine, *Biomacromolecules*, 2021, **22**, 1091–1101, DOI: 10.1021/acs.biomac.0c01467.

94  Z. Zhang, Y. Nie, Q. Zhang, X. Liu, W. Tu, X. Zhang and S. Zhang, *ACS Sustainable Chem. Eng.*, 2017, **5**, 2614–2622.

95  A. Franco-Vega, A. López-Malo, E. Palou and N. Ramírez-Corona, *Chem. Eng. Process.*, 2021, **160**, 108277.

96  Y. Qin, X. Lu, N. Sun and R. D. Rogers, *Green Chem.*, 2010, **12**, 968–971.

97  A. C. Dumetz, A. M. Chockla, E. W. Kaler and A. M. Lenhoff, *Biochim. Biophys. Acta*, 2008, **1784**(4), 600–610.

98  M. Kaya, T. Baran, I. Saman, M. A. Ozusaglam, Y. S. Cakmak and A. Menteşet, *J. Crustacean Biol.*, 2014, **34**, 283–288.

99  E. S. Abdou, K. S. A. Nagy and M. Z. Elsabee, *Bioresour. Technol.*, 2008, **99**, 1359–1367.

100  F. A. Sagheer, M. A. Al-Sughayer, S. Muslim and M. Z. Elsabee, *Carbohydr. Polym.*, 2009, **77**, 410–419.

101  M. K. Jang, B. G. Kong, Y. I. L. Jeong, C. H. Lee and J. W. Nah, *J. Polym. Sci., Part A: Polym. Chem.*, 2004, **42**, 3423–3432.

102  G. Nansé, E. Papirer, P. Fioux, F. Moguet and A. Tressaud, *Carbon*, 1997, **35**, 175–194.

103  J. M. Spörl, A. Ota, R. Beyer, T. Lehr, A. Müller, F. Hermanutz and M. R. Buchmeiser, *J. Polym. Sci., Part A: Polym. Chem.*, 2014, **52**, 1322–1333.

104  J. L. Shamshina, G. Gurau, L. E. Block, L. K. Hansen, C. Dingee, A. Walters and R. D. Rogers, *J. Mater. Chem. B*, 2014, **2**, 3924–3936.

105  C. Y. Soon, Y. B. Tee, C. H. Tan, A. T. Rosnita and A. Khalina, *Int. J. Biol. Macromol.*, 2018, **108**, 135–142.

106  E. C. Achinivu, J. L. Shamshina and R. D. Rogers, *Fluid Phase Equilib.*, 2022, **552**, 113286.

107 According to the Global Harmonized System (GHS) which has five categories for acute toxicity, the substance belongs to the lowest toxicity category 5 ($LD_{50}$ > 2000 mg $kg^{-1}$ < 5000 mg $kg^{-1}$, https://www.epa.gov/sites/production/files/2015-09/documents/ghscriteria-summary.pdf, accessed 26 February 2025.

108 Reach substance information ( https://echa.europa.eu/registration-dossier/-/registered-dossier/25928) 161, 249–265. 11 December, 2024.

109 S. Ostadjoo, P. Berton, J. L. Shamshina and R. D. Rogers, *Toxicol. Sci.*, 2018, **161**, 249–265.